Published in final edited form as:
J Med Chem. 2009 October 8; 52(19): 5967–5973. doi:10.1021/jm9006142.

Discovery of Novel Types of Inhibitors of S-Adenosylmethionine Synthesis by Virtual Screening

John C. Taylor, **Charles W. Bock**[≠,‖], **Fusao Takusagawa**[§], and **George D. Markham**[*,§]

[≠] Institute for Cancer Research, Fox Chase Cancer Center, 333 Cottman Avenue, Philadelphia, PA 19111

[§] Department of Molecular Biosciences University of Kansas, 1200 Sunnyside Avenue, Lawrence, KS 66045-7534

[‖] Department of Chemistry and Biochemistry, School of Science and Health, Philadelphia University, School House Lane and Henry Avenue, Philadelphia, PA 19144

Abstract

S-adenosylmethionine (AdoMet) lies at an intersection of nucleotide and amino acid metabolism, and performs a multitude of metabolic functions. AdoMet formation is catalyzed by S-adenosylmethionine synthetase (ATP : L-methionine S-adenosyltransferase (MAT)) which is a target for development of anti-cancer and antimicrobial agents. High affinity MAT inhibitors have been found through computational docking of more than 200,000 compounds for predicted binding to the crystallographically-defined nucleotide binding region of the enzyme's active site. Two of the top scoring candidate compounds had IC_{50} values less than 10 nM,, more than 10,000-fold lower than the substrates' K_M values. The compounds are structurally unrelated to the natural ligands of the enzyme. The enzyme is protected from inhibition by ATP, but not by methionine, consistent with binding at the adenosyl region of the active site. These results validate *in silico* screening as a robust approach to the discovery of inhibitors of this chemotherapeutically relevant enzyme.

INTRODUCTION

S-adenosylmethionine (AdoMet) has a central role in the life of all cells, joining the pivotal processes of nucleotide and amino acid metabolism.[1-4] AdoMet acts as methyl donor to DNA, RNA, proteins and small molecules, as a propylamine donor in the synthesis of the polyamines, as a 5′-deoxy-adenosyl free radical progenitor in a diverse family of “Radical SAM” enzymatic reactions, and has other specialized roles such as participation in the syntheses of hypermodified nucleotides in tRNA and the unusual amino acid hypusine. The roles of DNA and protein methylation in the epigenetic regulation of mammalian cell growth and differentiation have closely tied AdoMet to carcinogenesis.[5, 6]

S-adenosylmethionine biosynthesis involves the condensation of ATP and L-methionine which is catalyzed by S-adenosylmethionine synthetase (ATP: L-methionine S-adenosyltransferase, MAT).[7] Alterations in the abundance of the two MAT isozymes in hepatic diseases have led to an enduring search for specific inhibitors of potential use in cell biological studies and as potential chemotherapeutic agents.[8-15] More recently MAT has been proposed as a target for

§ Correspondence and proofs to: George D. Markham, Ph.D., Institute for Cancer Research, Fox Chase Cancer Center, 333 Cottman Avenue, Philadelphia, PA 19111; Telephone: 215-728-2439; Fax: 215-728-3574. GD_Markham@fccc.edu. * Address correspondence to George D. Markham, Ph.D., Institute for Cancer Research, Fox Chase Cancer Center, 333 Cottman Avenue, Philadelphia, PA 19111. Tel: 215-728-2439. Fax: 215-728-2412. gd_markham@fccc.edu.

the development of anti-parasitic agents.16 However MAT's substrates, ATP and methionine, partake in numerous metabolic processes, thus generating specific, bioavailable, inhibitors as compounds that are structurally related to the substrates remains challenging. Furthermore MATs from eukarya and bacteria are generally highly conserved in sequence and structure, particularly in residues comprising the active site, further suggesting a difficult inhibitor design problem.[17] Nevertheless numerous analogs of the substrate methionine have been synthesized as potential MAT inhibitors.[8-14, 18-24] Some of the methionine analogs, particularly L-*cis*-AMB (L-2-amino-4-methoxy-*cis*-but-3-enoic acid10) and the commercially available cycloleucine (1-amino, 1-carboxy-cyclopentane), have had biological applications because of their ability to enter cells, despite their at best micromolar affinity for MAT and their unclear effects on other amino acid utilizing enzymes.[8, 12, 13] Bi-substrate analogs that link portions of methionine to the 5′ position of the nucleotide substrate have been prepared in complex syntheses;[14, 18-25] these compounds had K_i values in the low micromolar range and displayed some selectivity between rat MAT isozymes, however these scarce inhibitors have had limited application. This laboratory has described the potent, mechanism-based, inhibition of MAT by diimidotriphosphate (O_3P-NH-PO_2-NH-PO_3; PNPNP) a non-hydrolyzable analog of the tripolyphosphate reaction intermediate with a 2 nM dissociation constant for the *E. coli* MAT.[15] However PNPNP had no effects on the growth of *Escherichia coli*, *Saccharomyces cerevisiae* or the NCI 60-cell line panel, likely due to its highly charged nature, formally −5 at neutral pH (unpublished results).

The present work describes the identification of the first MAT inhibitors that are structurally unrelated to the reactants, intermediate or products of the enzyme. In a new approach for this enzyme, we have taken advantage of the availability of the crystal structure of the MAT from *E. coli*,[26, 27] and have used computational docking to screen libraries of commercially available compounds for predicted binding to the enzyme's active site. Experimental tests of a limited selection of candidate compounds verified two potent inhibitors of the enzyme with IC_{50} values near 10^{-9} M, more than 10,000-fold lower than the K_M for either substrate.[28]

RESULTS

Virtual screening of ca. 200,000 compounds as potential ligands to the active site of MAT from *E. coli*, followed by visual inspection of the docked poses of ~200 of the best scoring inhibitors, has led to the identification of two potent inhibitors (**1** and **2**, each illustrated schematically and in their predicted binding conformation in Figure 1). Eight compounds were selected for experimental testing based on both their predicted affinity (i.e. their Glide Scores) and the predicted structures of their enzyme-bound complexes (Figure 2), however only five of them were available. The method of selection relied upon the prediction of hydrogen bonding to key active site ligands (see below) and interaction with the sole aromatic active site residue, phenylalanine-230. Two compounds provided complete inhibition of MAT activity at a concentration of 1 mM in initial tests, and were then characterized in detail (see **Methods**). The other compounds did not cause detectable inhibition at 1 mM concentrations and were not further investigated. The binding poses predicted by Glide for **1** and **2**, which we propose to be denoted AntiMAT-1 and AntiMAT-2 respectively, are illustrated in Figure 2. The poses predict hydrogen bonding to Histidine-14, Lysine-265, and Aspartate-271 which are key residues in binding and catalysis, and both compounds have a nitrophenyl moiety which is predicted to stack with Phenylalanine-230 upon which the adenine ring of the substrate normally lies.[29]

Measurements of enzyme activity at various inhibitor concentrations revealed that at the micromolar enzyme concentrations used for activity measurements there was complete inhibition by approximately equimolar concentrations of either **1** or **2** and the protein (Figure 3). The dependence of residual enzyme activity on ligand concentration was fit to the equation

for tight-binding inhibition (i.e. one where the K_i value is comparable to the protein and inhibitor concentrations used in the experiments, see **Methods**). These analyses (Figures 3A and 3B) reported K_i values of 1.9 ± 0.8 nM and 6.9 ± 2.1 nM for **1** and **2**, respectively. Figures 4A and 4B show that when 10 mM ATP was included during an incubation of enzyme and ligand, and aliquots were removed for activity determination by addition of methionine, no inhibition was observed with either compound. In contrast when 1 mM methionine (the highest concentration compatible with the activity assay) was included in the incubation of enzyme and ligand (before addition of ATP to start the assay) the same degree of inhibition was observed as in the absence of methionine.

The inhibition by both **1** and **2** has a slow onset, consistent with the high affinities and slow dissociation rates (see below). At 200 μM **1** and 10 μM enzyme, half-maximal maximal inhibition was achieved in ca. 7 min., corresponding to a rate of 1.6×10^{-3} s^{-1}, see Figure 4C. A similar experiment with **2** revealed a half time of 20 min. A limit on the dissociation rate of the Enzyme•AntiMAT complexes was estimated from the lack of recovery of detectable activity after a 24 hr dialysis of a mixture of enzyme and either inhibitor against 1250 volumes of buffer (enzyme and inhibitor were initially present at 0.25 μM and 0.3 μM, respectively; if equilibrated, the final concentration of inhibitor would have been 0.25 nM). An estimate of the dissociation rate was obtained from the limit of detection of 10% recovery of the enzyme activity, from which the off rate was estimated as $< 3 \times 10^{-6}$ s^{-1}. (at 4° C where the dialysis was conducted). For **1**, a dissociation rate of ~10^{-6} s^{-1} can be estimated from the 1.6×10^{-3} s^{-1} rate of inhibition onset and the 1.9 nM K_i value. An analogous analysis indicates a similar dissociation rate for **2**.

Inhibitor Specificity

1 and **2** were tested for potential inhibition of the MAT homolog from the archaeon *M. jannaschii*, which has less than 20% sequence identity to the *E. coli* MAT and for which protein circular dichroism spectra indicate a structure that is likely to be different (a crystal structure is not available for this protein or a close relative).[30] At concentrations up to 1 mM neither compound inhibited the archaeal *M. jannaschii* enzyme, even after a 20 min preincubation with the protein before activity measurement (see Methods).

Potential Cell Growth Inhibition

We examined whether either of **1** or **2** inhibited the growth of either *Saccharomyces cerevisiae* or *E. coli* on solid media by placing a filter disk that was soaked with either 1 mM candidate compound dissolved in DMSO, or a DMSO control, on a freshly spread lawn of cells. No inhibition was observed in any case. Since labeled compounds were not available, we could not determine whether they were taken up by the cells and thus could become available to the cytosolic MAT. In addition both **1** and **2** were evaluated by the Developmental Therapeutics Program of the National Cancer Institute for potential inhibition of the growth of their panel of 60 mammalian tumor cell lines (http://dtp.nci.nih.gov/branches/btb/ivclsp.html);[31, 32] concentrations up to 100 μM were tested. Neither compound caused detectable growth inhibition of any of the cell lines; as in the case of the trials with *E. coli* and yeast, it was not possible to determine whether the compounds were transported into the cells which would be required for MAT inhibition.

DISCUSSION

The present report describes success in finding novel types of MAT inhibitors by an initial virtual screen, docking several hundred thousand compounds to the active site of cMAT, followed by experimental evaluation of a restricted number (5) of candidates which were selected by visual inspection of the poses of the best scoring compounds. The two new

inhibitors are structurally distinct from the natural ligands and may provide useful leads to novel bioavailable inhibitors. The success rate of this screen was atypically good; for example we recently reported the discovery of one compound that stabilizes a minor hexameric assembly of the predominantly octameric porphobilinogen synthase upon experimental testing of 76 candidates identified by using *Glide* to screen ca. 60,000 compounds from a different library of candidate ligands for potential binding to a postulated inter-subunit interfacial binding site;[33] in that case the success rate may be abnormally low because the site chosen was an adventitious location formed upon hexamer assembly rather than an evolved ligand binding site. The reason for our current high success rate may also be related to the small and highly polar nature of the enzyme's active site, which is lined with 4 cationic residues and 3 anionic residues and to which 2 Mg^{2+} ions and a K^{+} ion bind as well as the substrates.[26, 27] These ionic protein residues may select for the binding of compounds that can have several directional interactions (e.g. hydrogen bonds) that are complimented by stacking with Phenylalanine-230, the sole aromatic residue at the active site. It should be noted that an experimental search of a library of this magnitude for MAT inhibitors could not have been easily performed using the standard assay methods, not only due to the cost of assembling the library of candidate ligands, but also the precautions in handling the radioactive materials, the cost of ^{14}C labeled substrates, and the disposal of radioactive waste.

The two MAT inhibitors described herein did not inhibit cell growth in the systems tested. Nevertheless these inhibitors may provide scaffolds upon which to develop compounds with more desirable properties. Most importantly their discovery validates docking as a satisfactory method for the discovery of MAT ligands with unexpected structures.

COMPUTATIONAL METHODS

The libraries of structures of compounds that were to be screened for candidate inhibitors were obtained in SDF or Mol2 format from the Sigma-Aldrich Rare Chemical Library, Fluorous Technologies, Lancaster Chemicals, Maybridge Chemicals, and Peakdale Chemicals. These docking libraries were largely prepared before the announcement of the ZINC compendium;[34] while ZINC and our collection overlap, the differences in the processing of the structures to make them “dockable” will make the runtime libraries vary in the diverse structures that are present, even when the same 2-dimensional representations were initially used.

Modeling software from Schrödinger L.L.C. (New York, NY) was used throughout. The structures were obtained as two-dimensional representations typically without hydrogens and without designations of stereochemical configuration at chiral centers. Perl scripts were used to add appropriate hydrogen atoms to each compound, and the resultant structures were converted to a geometry-optimized, three-dimensional representation using the program MacroModel with the Merck Molecular Force field (MMFF) and the GB/SA continuum solvation model for water.[35, 36] Compounds that did not successfully energy minimize, due for example to atoms that were not represented in MMFF (e.g. metal ions), were of necessity discarded. This procedure generated a single representation of each starting structure. The structures were then expanded to include all ionization states predicted to be present at neutral pH using the Ionizer utility from Schrödinger, followed by repetition of the geometry optimization. The resulting combined library had ~200,000 structures.

The MAT protein structure was taken from the coordinates of the enzyme•ADP•Pi complex deposited in the Protein Data Bank (PDB code 1mxb, 2.80 Å resolution). 26 Since six amino acid residues that form an active site lid are disordered in this structure, the low energy conformer from our previous loop modeling work was used;37 these lid residues do not directly contact the substrates (or potential inhibitors) and do not intrude into the active site, unlike their positions in the crystal structure of the apo enzyme.26 All ligands and metal ions were

removed from the protein structure before further manipulation. The protein structure had been prepared to have side chains in their appropriate ionization states at neutral pH and had been energy minimized using the AMBER force field in the course of loop modeling.37 In order to enhance the conformity of the protein with the OPLS-AA force field used for docking by Glide, 38 the protein structure was subjected to a restrained energy minimization using the OPLS-AA(2001) force field39 the crystallographically defined heavy atoms were allowed to deviate from up to 0.3 Å from their experimental positions without energy penalty, beyond which a 100 kJ/mol-Å^2 penalty was applied, as in our previous work.[37]

The docking protocol used the program Glide (version 2.0) from Schrödinger, L.L.C, (New York, NY, 2005).[38,] 40 A 16 Å^3 box centered on the ADP ligand was chosen as the region which the ligand center must occupy, and a larger 30 Å^3 box was used to define the region in which the entire docked ligand must lie. Glide allows the ligand to have fully flexible torsional geometry, but retains the bond lengths and angles of the input structure; hence it was important to have optimized the geometries of the ligand structures before docking. A 'soft' protein surface in which the van der Waals radii of the polar protein atoms were reduced by a factor of 0.8 was used to simulate protein malleability. The van der Waals radii of the ligands were also reduced by a factor of 0.8 for a similar reason. Several crystal structures of *E. coli* MAT have shown that the ATP binding site accepts differing nucleotide conformations while enzymatic activity retains substantial specificity for the adenosine moiety; for example, a comparison of the positions of the nucleoside moiety in the complex with ADP and P_i (originating from hydrolysis of ATP during the crystallization, pdb code 1m×b)26 with that observed in a complex with both substrate sites occupied (by the ATP analog AMPPNP and methionine, pdb code 1p9l)29 shows that while the phosphoryl groups occupy analogous locations the adenosine moiety swaps position between alternate sites located near either end of the phosphate chain, depending in part on the presence of the methionine co-substrate).29

The output of Glide docking is a list of compounds ranked by "Glide Score" which is a modified version of Chemscore,41 with units of kcal/mol. In order to estimate the Glide Scores that might be expected for potent inhibitors, and to evaluate the reliability of ligand positioning, we first docked the product AdoMet which forms a complex for which the crystal structure has been determined (pdb code 1rg9).26 The 3 μM dissociation constant of AdoMet is the lowest of any compound known to bind without complex kinetics.7 Glide positioned AdoMet with a heavy atom rmsd of 1.1 Å from the crystallographically determined location,29 indicating reliable docking. We choose a cutoff for further evaluation of the candidate ligands as those which docked with poses (poses being defined as the combination of ligand conformation and position) having Glide Scores at least 2 kcal/mol lower (predicted higher affinity) than the Glide Score of AdoMet (−6.5 kcal/mol). Only 10% of the library docked with Glide Scores better than AdoMet, and only 0.08% (170 structures) docked with Glide Scores less than −8.5 kcal/mol. The docked poses of the compounds passing this criterion were then visually examined, and a small selection of compounds which were predicted to cover a significant portion of the active site were chosen for experimental evaluation.

EXPERIMENTAL METHODS

Reagents were acquired from Sigma-Aldrich except where noted. MAT from *E. coli* (cMAT) was isolated from an overproducing strain as described previously.[15] cMAT concentrations were based on the UV absorbance at 280 nm using an extinction coefficient of 1.3 (mg/ml-cm)$^{-1}$ and a subunit molecular mass of 41941 Daltons. Purified recombinant MAT from the archaeon *Methanococcus jannaschii* was obtained from Dr. Z. Lu of this laboratory.[30] The concentration of MJ-MAT was determined from UV absorbance at 280 nm using an extinction coefficient of 1.0 (mg/ml-cm)$^{-1}$ and a subunit molecular mass of 45252 Daltons.[30]

A group of compounds that were identified from the docking screen as possible inhibitors were purchased from the Sigma-Aldrich Rare Chemical Library and their identifying catalog numbers are given along with their chemical names and Chemical Abstracte Service (CAS) Registry Number. These were: **1**, S903566, (1-(3-(2-ethoxyphenyl)ureidoacetyl)-4-(2-methyl-5-nitrophenyl)semicarbazide, CAS Registry Number 198704-90-4); **2**, S867349, (1-(4-chloro-2-nitrophenyl)-3-(4-sulfamoylphenyl)urea), CAS Registry Number 197160-37-5; **3**, S702633, 1,1′-((2-chlorobenzyl)-2-methylphenylene)bis(3-antipyrinylurea), CAS Registry Number 883838-93-5; **4**, S720844, 1-(4-methyl-2-nitrophenyl)-3-(4-sulfamoylphenyl)urea, CAS Registry Number 200347-89-3; and **5**, S890901, 1,1′-(4-Methyl-1,3-Phenylene)Bis-(3-(3-(Trifluoromethyl)phenyl)urea), CAS Registry Number 200416-79-1.

MAT activity determinations measured incorporation of L-[methyl-^{14}C]-methionine (Moravek Biochemicals) into AdoMet, which was absorbed onto Whatman P-81 cation exchange filter paper and quantified by scintillation counting of the filters after extensive washing with water.[15] Routine activity measurements utilized 50 mM Tris•Cl, 50 mM KCl, 10 mM $MgCl_2$, 10 mM ATP, 0.5 mM L-[methyl-^{14}C]-methionine, pH 8.0. Typically reactions were allowed to proceed for 5 min at 25° C before quenching by the addition of 3 volumes of a 25 mM EDTA (pH 8.0) stop solution.

Inhibitor Characterization

Candidate inhibitors were dissolved in 100% dimethyl sulfoxide (the final amount of DMSO in the assays was maintained at 15% (by volume) unless otherwise noted). Control experiments showed that 15% DMSO did not affect the enzyme activity, either when included with the enzyme for up to an hour before activity measurement, or when it was present during the assay period.

Initial inhibitor screening assays contained reduced substrate concentrations of 0.1 mM ATP and 0.1 mM L-[methyl-^{14}C]-methionine; these substrate concentrations approximate their K_M values (0.11 mM for ATP and 0.08 mM for L-methionine).[42] Assays were conducted at 25° C, typically for a 5 - 10 min incubation period after initiation by addition of enzyme; assays were terminated by addition of an excess of 25 mM EDTA, pH 8.0. Product formation was linear with time for all assay protocols used. The *M. jannaschii* MAT was assayed using the same method but reactions were conducted at 37° C due to the low activity of this thermophilic enzyme at 25° C; the K_M values of *M. jannaschii* MAT were 0.29 mM for ATP and 0.24 mM for L-methionine.[30]

Since we had previously observed a slow onset of MAT inhibition by intermediate and product analogs,[15] possible inhibition was evaluated after a 20 min preincubation of the candidate inhibitor at either 0.2 mM or 1 mM with enzyme (0.25 μM) before addition of 1.5 volumes of concentrated assay reagents (final concentrations as above). Experiments were also performed in which the reactions were initiated by addition of enzyme to a solution containing substrates and candidate inhibitor to yield the same final concentrations.

In typical inhibitor screening, cMAT was preincubated at room temperature for 20 min. in 50 mM Tris•Cl pH 8.0, 50 mM KCl, 20 mM $MgCl_2$ with the indicated amount of potential inhibitor or a 15% DMSO control. The protein plus inhibitor solution was then mixed with 1.5 volumes of the assay reagents (final concentrations 50 mM Tris•Cl, pH 8.0, 50 mM KCl, 10 mM $MgCl_2$, 0.1 mM ATP, 0.1 mM [Methyl-^{14}C]-L-methionine) and the reaction was allowed to proceed for 5 min. at 25° C before quenching with 25 mM EDTA, pH 8.0, and followed by determination of the amount of AdoMet formed.

Kinetic data were fit to the equation for tight binding inhibition

$$v_{observed} = 1 - \left(([E] + [I] + K_i) - \left(([E] + [I] + K_i)^2 - (4^*[E]^*[I])^{0.5} \right) / (2^*[E]) \right)$$

where $v_{observed}$ is the fractional activity observed at a given concentration of enzyme and inhibitor, and [E] and [I] are the total concentrations of enzyme and inhibitor, respectively. K_i is the inhibition constant which was determined by non-linear regression using SigmaPlot v. 10. (SPSS Inc.).

Specificity of Inhibition

Both **1** and **2** were tested as inhibitors of MJ-MAT (0.3 μM) at co ncentrations from 0.1 to 1.0 mM; enzyme activity was measured after a 20 min preincubation of enzyme plus inhibitor, as described above. No alteration in the enzyme activity was observed.

Lack of activity recovery upon dialysis

The reversibility of the inhibition by **1** and **2** was investigated by determining the enzyme activity at various times after dialysis of an enzyme plus inhibitor mixture. A solution containing inhibitor (0.3 μM) and enzyme (0.25 μM) in 50 mM Tris•Cl, pH 8.0, 10 mM $MgCl_2$, 10 mM KCl was initially incubated at room temperature for 20 min. A portion of this inhibited mixture was then dialyzed against 1250 volumes of 50 mM Tris•Cl pH 8.0, 10mM $MgCl_2$, 10 mM KCl at 4° C. Aliquots were removed after 5, 10, 20, 30, 40, 50 60, 70, and 80 min. and 24 hours, added to assay concoction, and the enzyme activity quantified in the usual fashion. A control in the absence of inhibitors showed no loss in enzyme activity through the time period of the experiment.

Confirmation of the Identity of 1 and 2

The structures and purity of compounds identified as MAT inhibitors were verified by LC-MS. Analyses were conducted on a Waters LC-MS system configured with a DeltaPak C-18 column (3.9 × 300 mm; 15 micron; 100 Å) using a Model 2545 binary gradient pump with the following series of detectors: a Model 3100 mass spectrometer (in positive electrospray ionization mode), a Model 2424 ELS (Evaporative Light Scattering) detector, and a Model 2487 UV detector (254 nm). Elution used a 20 ml gradient from a mixture of 95% water, 5% methanol, 0.05% TFA to a final solution of 95% methanol, 5% water, 0.05% TFA at a flow rate of 0.8 ml per minute.

Reversed phase HPLC chromatograms of **1,** S9035666,,showed the same lone peak eluting at 16.28 min in each detection mode. The purity was estimated as ≥ 97% based on the integrated peak areas. The mass was reported as 430.2 (predicted 430.4; $C_{19}H_{22}N_6O_6$). UV/visible λ_{max} = 342 nm in DMSO. ^{1}H NMR (600 MHz, D_6-DMSO): 10.04 (s, 1H); 8.61 (s, 1H); 8.31 (s, 1H); 8.06 (s, 1H); 8.03 (m, 1H); 7.84 (m, 1H); 7.46 (d, J = 9.7 Hz, 1H); 7.42 (m, 1H); 6.93 (d, J=7.4 Hz, 1H); 6.84 (td, 7.4 Hz, 1.7 Hz, 1H); 6.78 (m, 1H); 4.07 (q, J=7.1 Hz, 2H); 3.84 (d, J = 5.4 Hz, 2H); 2.33 (s, 3H); 1.39 (t, 7.1 Hz, 3H).

Reversed phase HPLC chromatograms of **2**, S867349, ((1-(4-chloro-2-nitrophenyl)-3-(4-sulfamoylphenyl)urea), showed the same peak eluting at 14.15 min in each detection mode. The purity was estimated as ≥ 98% based on the integrated peak areas. The peak had a mass of 370.1 (predicted 370.7; $C_{13}H_{11}ClN_4O_5S$). UV/visible λ_{max} = 380 nm in DMSO. ^{1}H NMR (600 MHz, D_6-DMSO): 10.25 (s, 1H); 9.68 (s, 1H); 8.28 (d, J= 8.8 Hz, 1H); 8.15 (d, J = 2.0 Hz, 1H); 7.80 (dd, J = 2.0 Hz, 8.8 Hz, 1H); 7.75 (d, J = 8.8 Hz, 2H); 7.63 (d, J = 8.8 Hz, 2H); 7.25 (s, 2H).

Tests of Cell Growth Inhibition

1 and **2** were tested for their ability to inhibit the growth of *Escherichia coli* strain RP523 (*thr-1*, *leuB6*(Am), *fhuA21*, *lacY1*, *hemB220*, *glnV44*(AS), e14^{-}, *rfbC1*, *glpR200*(glp^{c}), *thi-1*) [43] which was obtained from Dr. Eileen Jaffe of the Fox Chase Cancer Center. RP523 is hyperpermeable to exogenous compounds, for example allowing entry of heme and conferring enhanced sensitivity to growth inhibition by antibiotics. Ca. 30 μl of an overnight cell culture were spread on a LB agar plate, and 5 mm diameter filter paper disks soaked with 30 μl of a 1 mM solution of MAT inhibitor or a DMSO control were placed on top. The size of the zone of growth inhibition was measured after an overnight incubation at 37° C.

Potential growth inhibition of *Saccharomyces cerevisiae* strain RDY84 (*MAT**a***, *pdr1ΔKAN*, *pdr3ΔHIS5+*, *ade2*, *trp1*, *his3*, *leu2*, *ura3*, *can1*) was investigated in an analogous fashion, using a growth temperature of 30° C on YDP agar plates. RDY84 was obtained from Dr. Warren Kruger of the Fox Chase Cancer Center.

The potential effects of **1** and **2** on the growth of the NCI-60 cell line panel were evaluated at the Division of Chemical Therapeutics of the National Cancer Institute.[32] Concentrations up to 100 μM were tested in their standard protocol.

Acknowledgments

This work was supported by National Institutes of Health Grants GM31186, CA06927, and also by an appropriation from the Commonwealth of Pennsylvania. The work was utilized the Fox Chase High Performance Computing Facility, the Organic Synthesis Facility and Research Secretarial Services. Helpful discussions regarding *Glide* with technical support persons at Schrodinger L.L.C. are gratefully acknowledged. We appreciate the help of Dr. Warren Kruger who contributed the yeast strain and provided advice on yeast growth, Dr. Trevor Selwood who aided in analysis of the tight binding kinetic data, and Dr. Eileen Jaffe for invaluable advice on many aspects of this study. We thank Dr. Hong Cheng for obtaining the NMR spectra and Cindy Myers for the HPLC and mass spectral analyses. We appreciate the help of Dr. Maxim Pimkin in preparing Figure 2. We thank the NCI Division of Chemical Therapeutics program for testing **1** and **2** for inhibition of the growth of the NCI-60 cell line panel.

Abbreviations

AdoMet	S-adenosylmethionine
cMAT	S-adenosylmethionine synthetase from *Escherichia coli*
MAT	S-adenosylmethionine synthetase (methionine adenosyltransferase)
MJ-MAT	S-adenosylmethionine synthetase from *Methanococcus jannaschii*
PNPNP	diimidotriphosphate (O_3PNH-PO_2-NH-PO_3)
AntiMAT-x	MAT inhibitor number “x” discovered in this work

REFERENCES

1. Cantoni GL. Biological methylation: selected aspects. Annu. Rev. Biochem 1975;44:435–451. [PubMed: 1094914]
2. Tabor CW, Tabor H. Polyamines. Annu. Rev. Biochem 1984;53:749–790. [PubMed: 6206782]
3. Markham, GD. Encyclopedia of Life Sciences. John Wiley & Sons, Ltd; London: 2003. S–Adenosylmethionine. Chichester http://www.els.net/ [DOI: 10.1038/npg.els.0000662]
4. Fontecave M, Atta M, Mulliez E. S-adenosylmethionine: nothing goes to waste. Trends Biochem. Sci 2004;29:243–249. [PubMed: 15130560]
5. Lu SC, Mato JM. S-Adenosylmethionine in cell growth, apoptosis and liver cancer. J. Gastroenterol. Hepatol 2008;23(Suppl 1):S73–S77. [PubMed: 18336669]

6. Mato JM, Martinez-Chantar ML, Lu SC. Methionine metabolism and liver disease. Annu. Rev. Nutr 2008;28:273–293. [PubMed: 18331185]
7. Markham GD, Pajares MA. Structure-function relationships in methionine adenosyltransferases. Cell. Mol. Life Sci 2009;66:636–648. [PubMed: 18953685]
8. Coulter AW, Lombardini JB, Sufrin JR, Talalay P. Structural and conformational analogues of L-methionine as inhibitors of the enzymatic synthesis of S-adenosyl-l-methionine. 3. Carbocyclic and heterocyclic amino acids. Mol. Pharmacol 1974;10:319–334. [PubMed: 4859493]
9. Goldberg B, Rattendi D, Lloyd D, Sufrin JR, Bacchi CJ. Effects of intermediates of methionine metabolism and nucleoside analogs on S-adenosylmethionine transport by *Trypanosoma brucei brucei* and a drug-resistant *Trypanosoma brucei rhodesiense*. Biochem. Pharmacol 1998;56:95–103. [PubMed: 9698093]
10. Sufrin JR, Lombardini JB, Keith DD. L-2-Amino-4-methoxy-cis-but-3-enoic acid, a potent inhibitor of the enzymatic synthesis of S-adenosylmethionine. Biochem. Biophys. Res. Commun 1982;106:251–255. [PubMed: 7103990]
11. Sufrin JR, Lombardini JB, Alks V. Differential kinetic properties of L-2-amino-4-methylthio-cis-but-3-enoic acid, a methionine analog inhibitor of S-adenosylmethionine synthetase. Biochim. Biophys. Acta 1993;1202:87–91. [PubMed: 8373829]
12. Lavrador K, Guillerm D, Guillerm G. A new series of cyclic amino acids as inhibitors of S-adenosyl L-methionine synthetase. Bioorg. Med. Chem. Lett 1998;8:1629–1634. [PubMed: 9873403]
13. Lavrador K, Allart B, Guillerm D, Guillerm G. A new series of S-adenosyl-L-methionine synthetase inhibitors. J. Enzyme Inhib 1998;13:361–367. [PubMed: 9793839]
14. Vrudhula VM, Kappler F, Hampton A. Isozyme-specific enzyme inhibitors. 13. S-[5′(R)-[(Ntriphosphoamino)methyl]adenosyl]-L-homocysteine, a potent inhibitor of rat methionine adenosyltransferases. J. Med. Chem 1987;30:888–894. [PubMed: 3572977]
15. Reczkowski RS, Markham GD. Slow binding inhibition of S-adenosylmethionine synthetase by imidophosphate analogues of an intermediate and product. Biochemistry 1999;38:9063–9068. [PubMed: 10413480]
16. Krasky A, Rohwer A, Schroeder J, Selzer PM. A combined bioinformatics and chemoinformatics approach for the development of new antiparasitic drugs. Genomics 2007;89:36–43. [PubMed: 17070005]
17. Sanchez-Perez GF, Bautista JM, Pajares MA. Methionine adenosyltransferase as a useful molecular systematics tool revealed by phylogenetic and structural analyses. J. Mol. Biol 2004;335:693–706. [PubMed: 14687567]
18. Porter CW, Sufrin JR, Keith DD. Growth inhibition by methionine analog inhibitors of S-adenosylmethionine biosynthesis in the absence of polyamine depletion. Biochem. Biophys. Res. Commun 1984;122:350–357. [PubMed: 6743338]
19. Kramer DL, Sufrin JR, Porter CW. Relative effects of S-adenosylmethionine depletion on nucleic acid methylation and polyamine biosynthesis. Biochem. J 1987;247:259–265. [PubMed: 3426538]
20. Kramer DL, Sufrin JR, Porter CW. Modulation of polyamine-biosynthetic activity by S-adenosylmethionine depletion. Biochem. J 1988;249:581–586. [PubMed: 3342030]
21. Lim H, Kappler F, Hai TT, Hampton A. Isozyme-specific enzyme inhibitors. 12. C- and N-methylmethionines as substrates and inhibitors of methionine adenosyltransferases of normal and hepatoma rat tissues. J. Med. Chem 1986;29:1743–1748. [PubMed: 3755757]
22. Kappler F, Vrudhula VM, Hampton A. Isozyme-specific enzyme inhibitors. 14. 5′(R)-C-[(L-homocystein-S-yl)methyl]adenosine 5′-(beta,gamma-imidotriphosphate), a potent inhibitor of rat methionine adenosyltransferases. J. Med. Chem 1987;30:1599–1603. [PubMed: 3498043]
23. Kappler F, Vrudhula VM, Hampton A. Toward the synthesis of isozyme-specific enzyme inhibitors. Potent inhibitors of rat methionine adenosyltransferases. Effect of one-atom elongation of the ribose-P alpha bridge in two covalent adducts of L-methionine and beta,gamma-imido-ATP. J. Med. Chem 1988;31:384–389. [PubMed: 3257524]
24. Kappler F, Hampton A. Approaches to isozyme-specific inhibitors. 17. Attachment of a selectivity-inducing substituent to a multisubstrate adduct. Implications for facilitated design of potent, isozyme-selective inhibitors. J. Med. Chem 1990;33:2545–2551. [PubMed: 2391695]

25. Kappler F, Hai TT, Cotter RJ, Hyver KJ, Hampton A. Isozyme-specific enzyme inhibitors. 11. L-homocysteine-ATP S-C5′ covalent adducts as inhibitors of rat methionine adenosyltransferases. J. Med. Chem 1986;29:1030–1038. [PubMed: 3486976]
26. Fu Z, Hu Y, Markham GD, Takusagawa F. Flexible loop in the structure of S-adenosylmethionine synthetase crystallized in the tetragonal modification. J. Biomol. Struct. Dyn 1996;13:727–739. [PubMed: 8723769]
27. Takusagawa F, Kamitori S, Markham GD. Structure and function of S-adenosylmethionine synthetase: crystal structures of S-adenosylmethionine synthetase with ADP, BrADP, and PPi at 28 angstroms resolution. Biochemistry 1996;35:2586–2596. [PubMed: 8611562]
28. A preliminary description of this work was present at the 2006 Federation of American Societies for Experimental Biology Meeting;
29. Komoto J, Yamada T, Takata Y, Markham GD, Takusagawa F. Crystal structure of the S-adenosylmethionine synthetase ternary complex: a novel catalytic mechanism of S-adenosylmethionine synthesis from ATP and Met. Biochemistry 2004;43:1821–1831. [PubMed: 14967023]
30. Lu ZJ, Markham GD. Enzymatic properties of S-adenosylmethionine synthetase from the archaeon *Methanococcus jannaschii*. J. Biol. Chem 2002;277:16624–16631. [PubMed: 11872742]
31. Gazdar AF, Minna JD. NCI series of cell lines: an historical perspective. J. Cell. Biochem. Suppl 1996;24:1–11. [PubMed: 8806089]
32. Marx KA, O'Neil P, Hoffman P, Ujwal ML. Data mining the NCI cancer cell line compound GI(50) values: identifying quinone subtypes effective against melanoma and leukemia cell classes. J. Chem. Inf. Comput. Sci 2003;43:1652–1667. [PubMed: 14502500]
33. Lawrence SH, Ramirez UD, Tang L, Fazliyez F, Kundrat L, Markham GD, Jaffe EK. Shape shifting leads to small-molecule allosteric drug discovery. Chem. Biol 2008;15:586–596. [PubMed: 18559269]
34. Irwin JJ, Shoichet BK. ZINC--a free database of commercially available compounds for virtual screening. J. Chem. Inf. Model 2005;45:177–182. [PubMed: 15667143]
35. Halgren TA. Merck molecular force field .1. Basis, form, scope, parameterization, and performance of MMFF94. J. Comput. Chem 1996;17:490–519.
36. Cheng A, Best SA, Merz KM Jr. Reynolds CH. GB/SA water model for the Merck molecular force field (MMFF). J. Mol. Graph. Model 2000;18:273–282. [PubMed: 11021543]
37. Taylor JC, Takusagawa F, Markham GD. The active site loop of S-adenosylmethionine synthetase modulates catalytic efficiency. Biochemistry 2002;41:9358–9369. [PubMed: 12135357]
38. Friesner RA, Banks JL, Murphy RB, Halgren TA, Klicic JJ, Mainz DT, Repasky MP, Knoll EH, Shelley M, Perry JK, Shaw DE, Francis P, Shenkin PS. Glide: a new approach for rapid, accurate docking and scoring. 1. Method and assessment of docking accuracy. J. Med. Chem 2004;47:1739–1749. [PubMed: 15027865]
39. Kaminski GA, Friesner RA, Tirado-Rives J, Jorgensen WL. Evaluation and reparametrization of th OPLS-AA force field for proteins via comparison with accurate quantum chemical calculations on peptides. J. Phys. Chem. B 2001;105:6474–6487.
40. Halgren TA, Murphy RB, Friesner RA, Beard HS, Frye LL, Pollard WT, Banks JL. Glide: a new approach for rapid, accurate docking and scoring. 2. Enrichment factors in database screening. J. Med. Chem 2004;47:1750–1759. [PubMed: 15027866]
41. Eldridge M, Murray CW, Auton TA, Paolini GV, Lee RP. Empirical scoring functions: I. The development of a fast empirical scoring function to estimate the binding affinity of ligands in receptor complexes. J. Comput.-Aided Mol. Des 1997;11:425–445. [PubMed: 9385547]
42. Markham GD, Hafner EW, Tabor CW, Tabor H. S-Adenosylmethionine synthetase from Escherichia coli. J. Biol. Chem 1980;255:9082–9092. [PubMed: 6251075]
43. Li JM, Umanoff H, Proenca R, Russell CS, Cosloy SD. Cloning of the *Escherichia coli* K-12 hemB gene. J. Bacteriol 1988;170:1021–1025. [PubMed: 3276659]

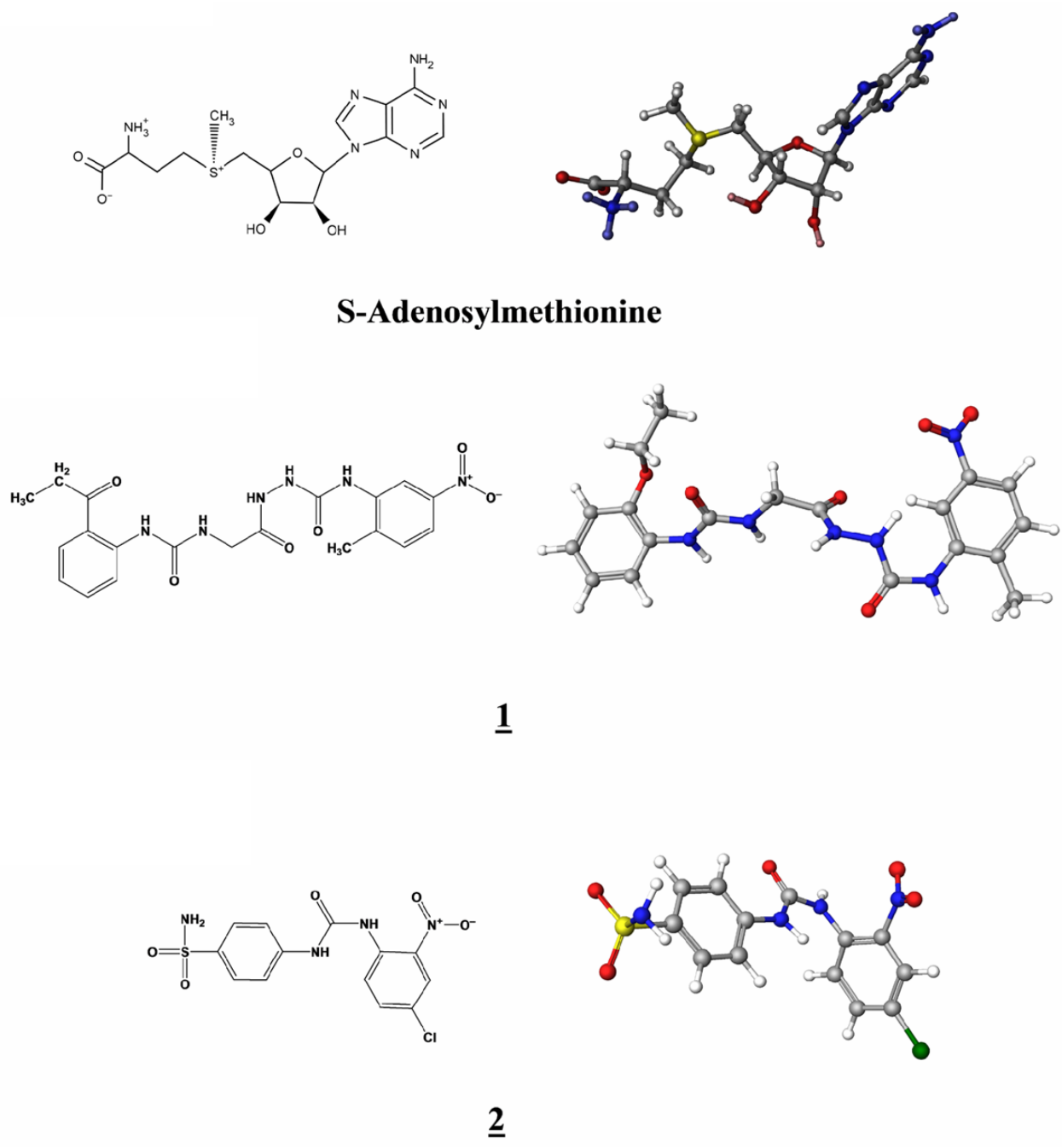

Figure 1.
The structures of AdoMet and the potent inhibitors identified by virtual screening. Part A, AdoMet. Part B, **1**, AntiMAT-1, and Part C, **2**, AntiMAT-2. The ligands in their docked conformations are shown next to the line drawings.

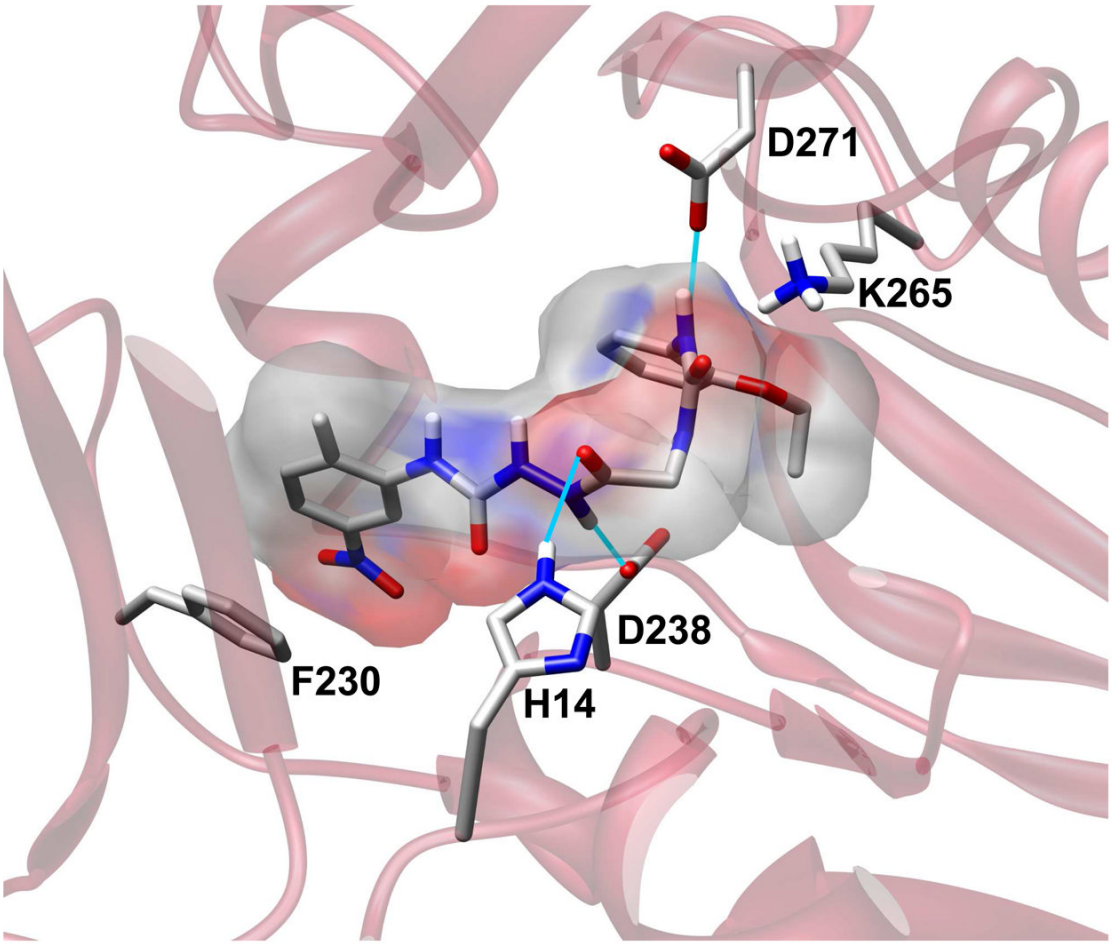

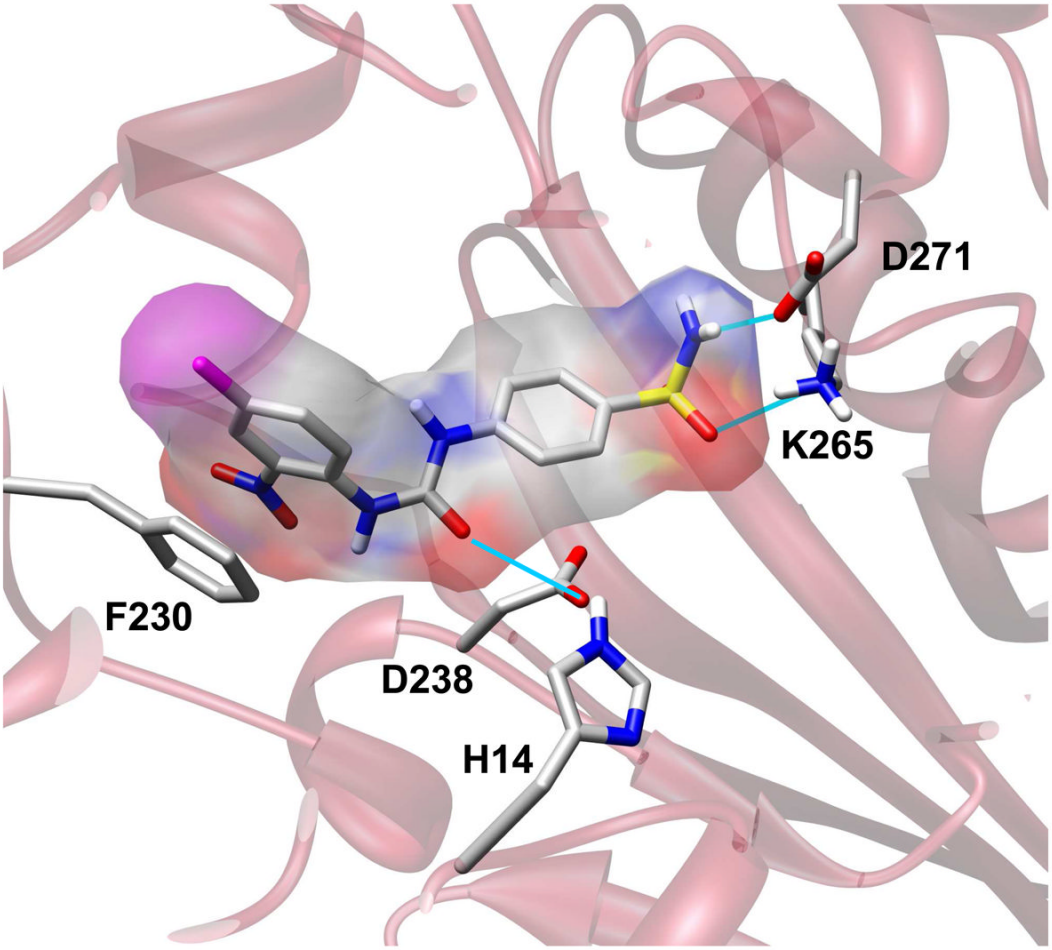

Figure 2.
Models of **1** and **2** docked into the active site of MAT taken from the crystal structure of the complex of the protein with ADP and Pi (pdb code 1mxb).[26], 27 Ligand conformations are those predicted by Glide38. Part A shows the predicted binding mode of **1** and Part B illustrates the predicted binding mode of **2**. Inhibitors are shown in ball-and-stick representation and the protein backbone as ribbons; Selected active site side chains predicted to interact with the inhibitors are illustrated. The surfaces of the ligands are shown colored by electrostatic potential.

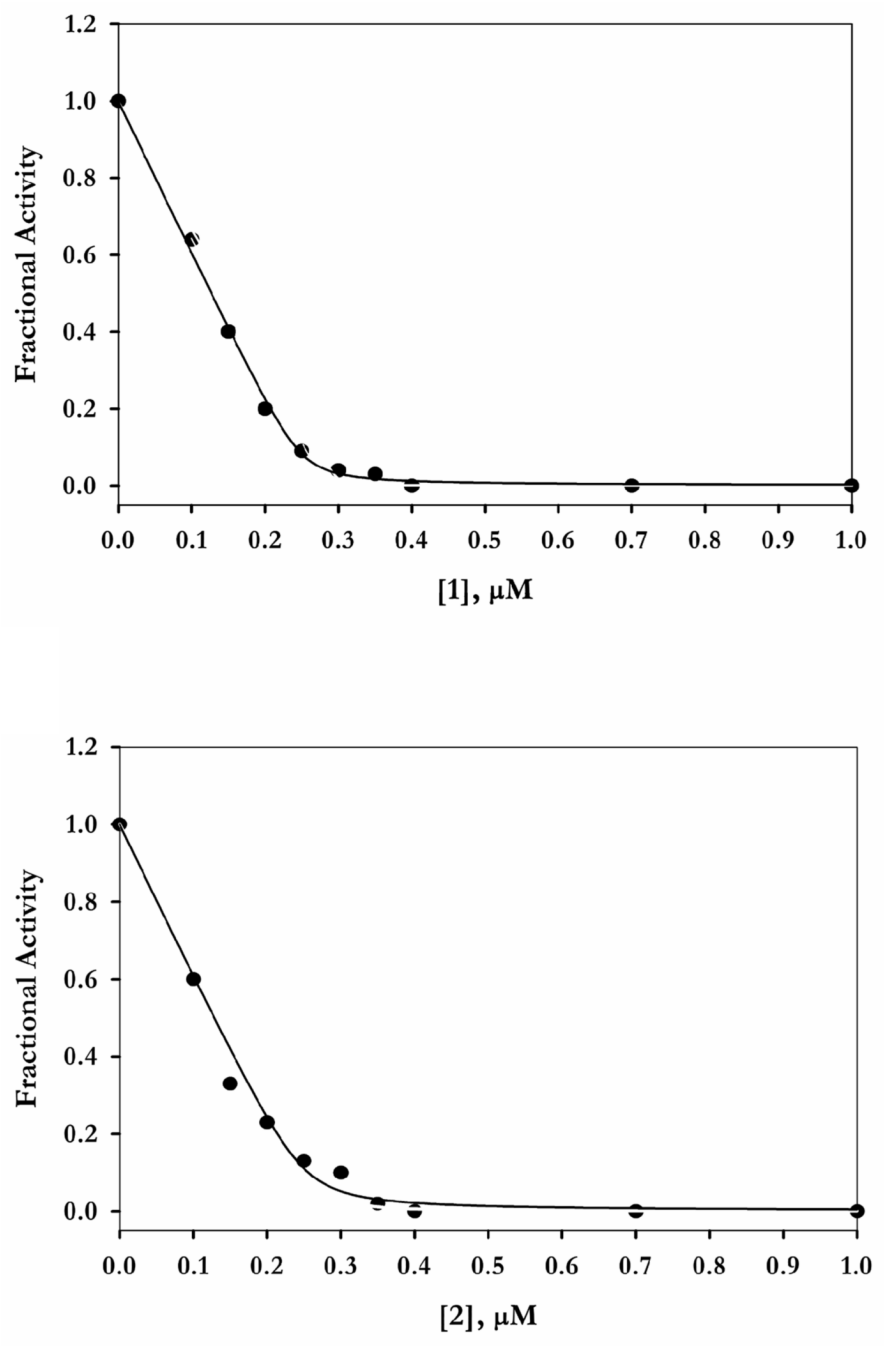

Figure 3.

Dependence of MAT activity on inhibitor concentration. Solutions contained various concentrations of **1** or **2** and 0.3 μM MAT subunits in 50 mM Tris•Cl, 50 mM KCl, 10 mM $MgCl_2$, 10 mM ATP, 0.5 mM L-methionine, pH 8.0, T = 25 °C. Enzyme and inhibitor were incubated together for 20 min before addition of substrates. Lines are fits of the data to the equation for tight binding inhibition (see **Experimental Methods)** with K_i values of 1.9 nM in Part A and 6.9 nM in Part B.

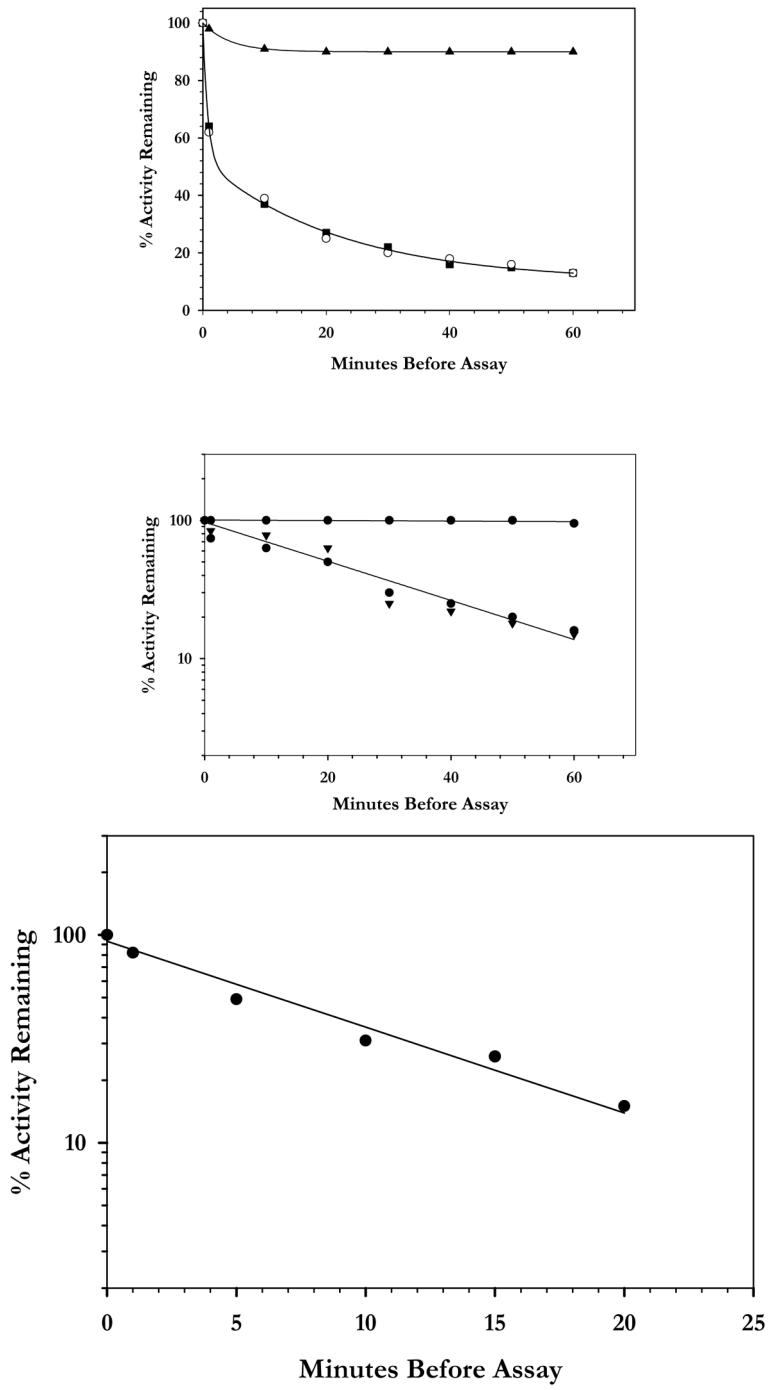

Figure 4.

Kinetics of the onset of inhibition by **1** illustrating protection by ATP but not by methionine. Part A shows inhibition by 0.3 μM **1**, whereas Parts B and C had 200 μM **2** and 200 μM **1**, respectively (note the log scale for activity in Parts B and C). Solutions contained 0.3 μM MAT subunits in Part A in 50 mM Tris•Cl, 50 mM KCl, 10 mM $MgCl_2$,. In Parts B and C the enzyme concentration was 10 μM. Where present the ATP and L-methionine concentrations were 10 and 1 mM respectively. Reactions were initiated by dilution of the enzyme•inhibitor mixture into assay reagents (see Methods).